

**Zeitschrift:** IABSE reports = Rapports AIPC = IVBH Berichte  
**Band:** 37 (1982)

**Artikel:** Fatigue and fracture analysis of defects in a tied arch bridge  
**Autor:** Fisher, John W. / Hausammann, Hans / Pense, Alan W.  
**DOI:** <https://doi.org/10.5169/seals-28953>

#### **Nutzungsbedingungen**

Die ETH-Bibliothek ist die Anbieterin der digitalisierten Zeitschriften auf E-Periodica. Sie besitzt keine Urheberrechte an den Zeitschriften und ist nicht verantwortlich für deren Inhalte. Die Rechte liegen in der Regel bei den Herausgebern beziehungsweise den externen Rechteinhabern. Das Veröffentlichen von Bildern in Print- und Online-Publikationen sowie auf Social Media-Kanälen oder Webseiten ist nur mit vorheriger Genehmigung der Rechteinhaber erlaubt. [Mehr erfahren](#)

#### **Conditions d'utilisation**

L'ETH Library est le fournisseur des revues numérisées. Elle ne détient aucun droit d'auteur sur les revues et n'est pas responsable de leur contenu. En règle générale, les droits sont détenus par les éditeurs ou les détenteurs de droits externes. La reproduction d'images dans des publications imprimées ou en ligne ainsi que sur des canaux de médias sociaux ou des sites web n'est autorisée qu'avec l'accord préalable des détenteurs des droits. [En savoir plus](#)

#### **Terms of use**

The ETH Library is the provider of the digitised journals. It does not own any copyrights to the journals and is not responsible for their content. The rights usually lie with the publishers or the external rights holders. Publishing images in print and online publications, as well as on social media channels or websites, is only permitted with the prior consent of the rights holders. [Find out more](#)

**Download PDF:** 04.02.2026

**ETH-Bibliothek Zürich, E-Periodica, <https://www.e-periodica.ch>**



## **Fatigue and Fracture Analysis of Defects in a Tied Arch Bridge**

Fatigue et analyse de la rupture des défauts dans un pont-arc avec tirant

Ermüdungs- und Bruchanalyse von Schäden an einer Stahlbogenbrücke mit Zugband

### **JOHN W. FISHER**

Professor  
Lehigh University  
Bethlehem, PA, USA

### **HANS HAUSAMMANN**

Research Engineer  
ICOM-Construction Métallique  
Lausanne, Switzerland

### **ALAN W. PENSE**

Professor  
Lehigh University  
Bethlehem, PA, USA

### **SUMMARY**

Cracks were detected in the corner weld of the box girders forming the tension members of the tied arch bridge over the Gulf Outlet in Louisiana. A fractographic examination of several cracked corner welds revealed that the cracks extended into the weld metal and heat-affected zone. An analysis of the fatigue and fracture behaviour of the cracks is provided.

### **RESUME**

Des fissures ont été détectées dans la soudure d'angle des poutres en caisson formant la membrure tendue du pont-arc avec tirant sur la „Gulf Outlet” en Louisiane. Un examen fractographique de plusieurs soudures d'angle fissurées a révélé que les fissures se propagent dans le métal de la soudure et dans la zone affectée par l'échauffement. Une analyse du comportement à la fatigue et à la rupture des fissures a été fournie.

### **ZUSAMMENFASSUNG**

In den Ecken der Kastenträger, die das Zugband der Bogenbrücke über den Golf von Outlet in Louisiana bilden, wurden Risse beobachtet. Die fraktographische Untersuchung mehrerer gerissener Eckschweissungen zeigte, dass sich die Risse in das Schweissgut und den durch Hitze beeinflussten Umgebungsbereich fortpflanzten. Eine Untersuchung des Ermüdungs- und Bruchverhaltens der Risse wird präsentiert.



## 1. INTRODUCTION

The tension members of several tied arch bridges consist of welded built-up sections. These sections are often welded box girders fabricated of single strength steel. High stresses due to the dead load and the live load are carried by these sections. These members are of major structural importance, because a fracture of a tie would likely result in a catastrophic failure of the bridge.

The Mississippi River Gulf Outlet Bridge is located near New Orleans, Louisiana. Figure 1 shows a view of the structure and a tie girder. The tie girders were fabricated of A514 steel. The suspended span is 170.7 m long, and the trusses are spaced 22.86 m apart.

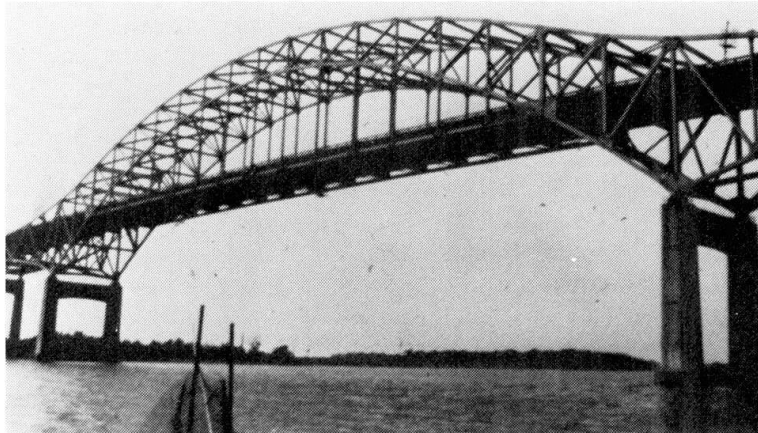


Fig. 1a Overview of Structure



Fig. 1b View of Tie Girder

The tie girders in the Gulf Outlet Bridge are box sections. The web plates are 711 mm high and 19 mm thick, the flanges are 635 mm wide and 16 mm thick. The plates are fillet welded at the four box corners. At floor beam connections and at the pinned connection of the tie (see Fig. 1b), additional interior corner welds are used to transfer the forces. The dimensions of the box are shown in Fig. 2.

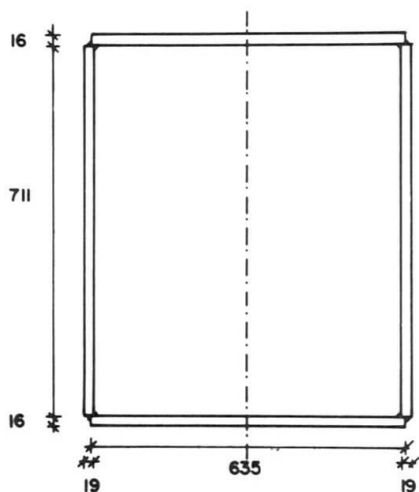


Fig. 2 Dimensions of Tie Girder (mm)

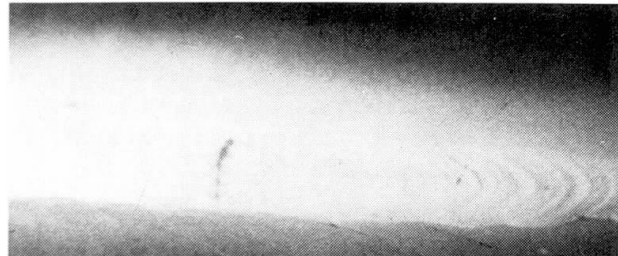


Fig. 3 Crack in Longitudinal Weld

Transverse cracking was inadvertently detected in the box corner fillet welds when the web groove welds at the pinned connection were being checked by radiography. Figure 3 shows one of the interior weld cracks after it was enhanced with liquid penetrant. Some cracks were below the surface and were only visible after slightly grinding the weld surface.

Several of the defects were removed from the box corners by coring (see Fig. 4a), so that detailed metallographic and fractographic studies could be carried out to ascertain the cause of cracking. Figure 4b shows the polished face of the box

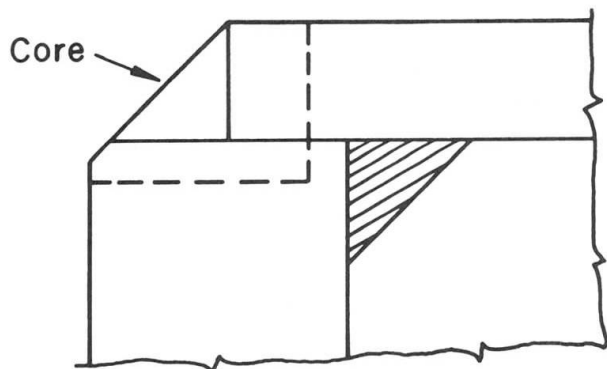


Fig. 4a Schematic Showing Core Sample at Web-Flange Corner Weld

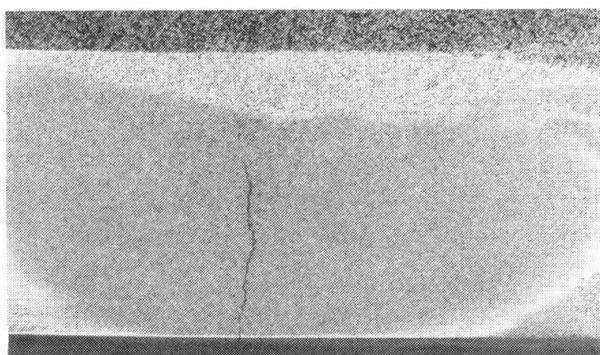


Fig. 4b Ground Surface of Weld Segment Showing Crack

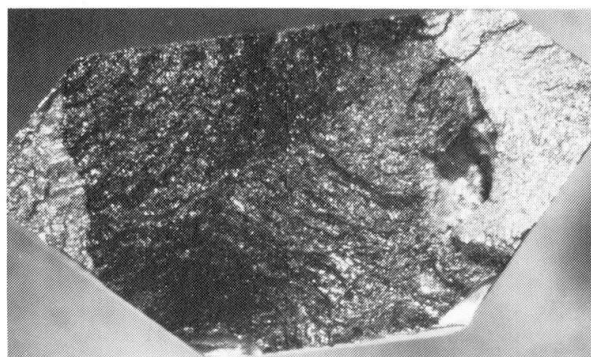


Fig. 4c Exposed Crack Surface

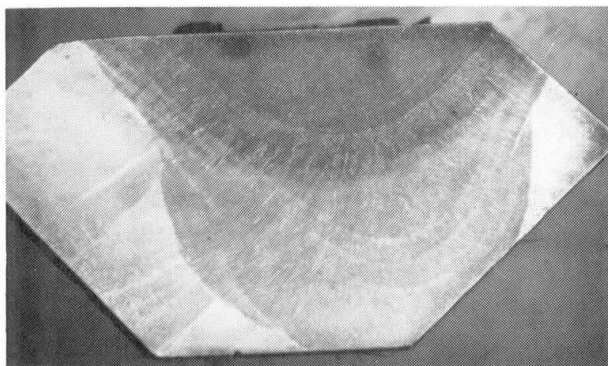


Fig. 4d Polished and Etched Surface Behind Crack

corner weld and the transverse weld crack that was observed. The small segment was broken open to expose the crack surface which is shown in Fig. 4c. A section just behind the crack surface was polished and etched and can be seen in Fig. 4d. This illustrates that multiple weld passes were added to the original submerged arc weld and that the crack extends throughout the corner weld into the heat-affected zone. On the whole, the fractographic examination of the crack surface suggested that the crack was produced during or shortly after welding. Some fatigue crack growth striations were also suggested in a few areas at very low  $\Delta K$  levels. Similar transverse weld cracking has been reported in groove welds and attributed to hydrogen and residual stresses<sup>1</sup>.

Because the cracks at the intersection between the web and the flange are oriented perpendicular to the main stress field due to the dead load and live load, an investigation was made to determine if these cracks could propagate under the cyclic live load stress. Small cracks may sharpen under cyclic load and also initiate brittle fracture, as a result of the high residual tensile stresses due to welding at the box corners.

## 2. STRESSES AT THE CRITICAL LOCATION

The bottom chord in a tied arch bridge is mainly subjected to high tensile forces due to the dead and live load and to residual stresses. The design calculations indicated a dead load stress of 252 MPa existed in the tie girder box of the Gulf Outlet Bridge. The dead load stress was assumed to be uniformly distributed over the cross-section.



The actual live load stress range was not known. The design live load stress range including an impact factor of 7.5%, is 48 MPa. Based on the design calculation and existing measurements on large bridge structures<sup>2,3</sup>, the Miner effective stress range was estimated to be 14 MPa, and the highest regularly encountered live load stress range is 28 MPa.

The residual stress due to welding the box corners was estimated using a procedure outlined in Ref. 4. To predict the residual stresses and strains, a finite discretization at the cross-section was used.

The calculation of the residual stresses assumed an elastic-perfectly plastic stress-strain response and temperature dependent material properties. The variation of the temperature as a function of the time and the location on the cross-section for each weld pass has to be known. It has been shown that the temperature distribution at discrete time intervals must be known in order to minimize the calculation efforts<sup>5</sup>.

The determination of the temperature distribution in the web and flange plate due to the heat input of welding is based on the principles of heat transfer in a thin semiinfinite plate. The temperature at a given location in the plate is a function of the heat input, the position of the location relative to the moving heat source (electrode) and various thermal properties of the plate. For the calculation of the temperature in the plates, the following assumptions were made<sup>6</sup>:

- Between 15 and 35% of the heat is lost, due to radiation and melting of the electrode,
- The temperature at some distance from the heat source remains unchanged,
- The heat source is a point source,
- The temperature is dependent on the distance between the heat source and the location of the point for which the temperature has to be predicted, and
- Half the heat produced by welding the web-flange connection goes into the web plate and half into the flange plate, independent of the thickness.

Different weld passes are made during the fabrication of the box girder. First, the plates are temporarily assembled with small tack welds. Then the automatic submerged arc welds at the outside corners are made. Next, longitudinal welds

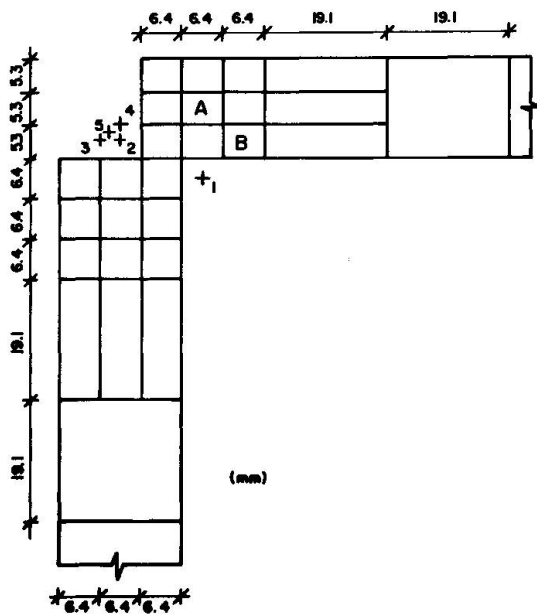


Fig. 5 Weld Sequence and Discretization near Box Corner Weld

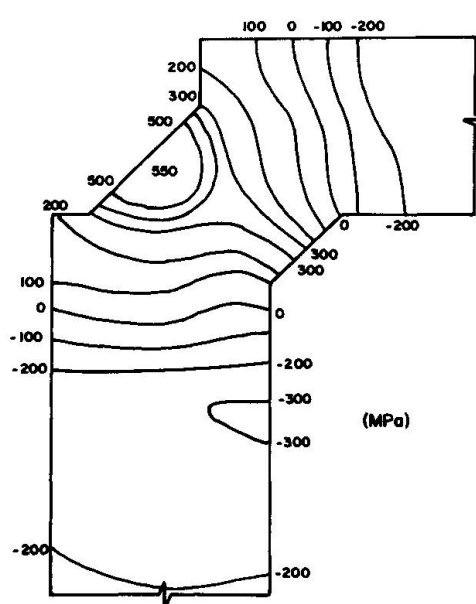


Fig. 6 Residual Stress Distribution near Box Corner Weld, Box Girder

inside the box are made manually, and finally several manual passes are made over the outside submerged arc weld. It is assumed that the total welding at one corner can be simulated with five weld passes.

The residual stresses due to welding were calculated using a computer program developed at the University of Missouri<sup>4</sup>. To calculate the stress distribution, the cross-section was divided into finite elements; part of the discretization is shown in Fig. 5, with the weld passes shown as crosses.

The residual stress distribution was calculated at the end of each weld pass. This distribution was used as the initial condition for the next weld pass. Based on the residual stress at the center of each element, the total distribution was derived using linear interpolation. The final stress distribution is shown in Figs. 6 and 7.

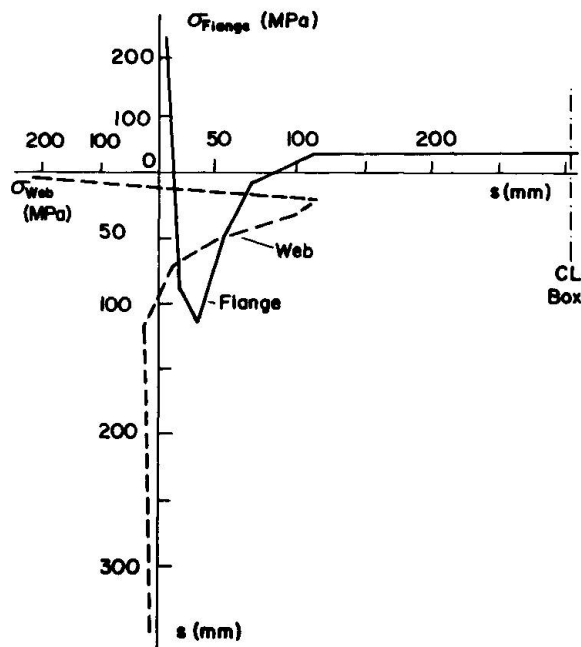


Fig. 7 Residual Stress Distribution due to Corner Welds in Middle Plan of Web and Flange Box Girder

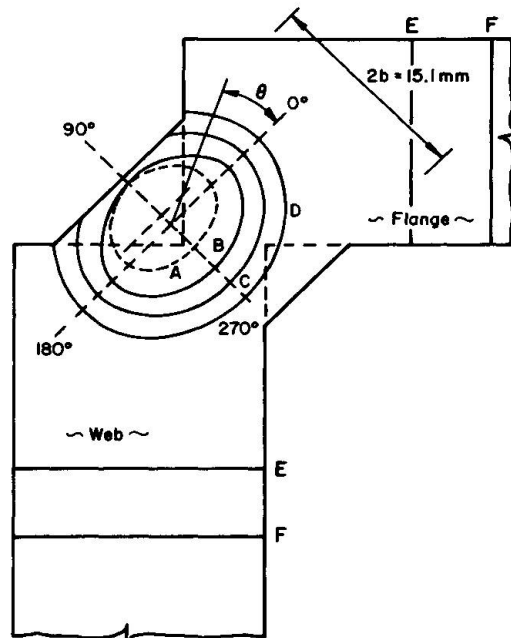


Fig. 8 Investigated Crack Shapes in Corner Weld, Box Girder

### 3. ANALYSIS OF THE CRACKS AT THE WELD CORNER

The cracks in the corner welds are of different shapes and sizes. Several shapes that were evaluated are shown in Fig. 8. It was assumed that the cracks can be analyzed as elliptical cracks circumscribing the flaw.

The total stress intensity factor is calculated using the principle of superposition. The K-value due to the uniformly applied dead and live load stress is calculated using the solution to an imbedded elliptical plan<sup>7</sup>. The K-value due to the residual stress shown in Fig. 7 was estimated using a procedure described in Ref. 8. The varying stress field is discretized by discrete point loads, and the corresponding K-value is calculated. The total K-value is obtained by an integration over the entire crack surface.

As the cracks are in the material of limited thickness, the K-factor has to be adjusted by the finite width and free surface correction factors.



All the cracks were close to the free surface. The material between the crack front and the weld surface is so thin, that it was easily ground away. This ligament is so small that it plastically deforms without initiating a brittle fracture. The load transmitted through this ligament is so small that it can be neglected. Instead of an internal elliptical crack, a U-shaped surface crack results.

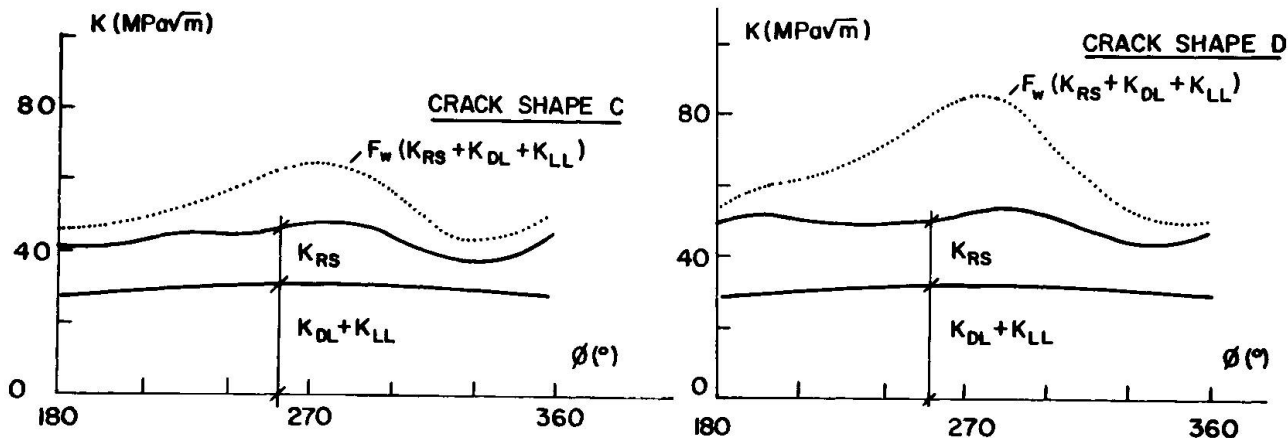


Fig. 9 Stress Intensity Factor for Cracks in Corner Weld

The crack shapes indicated in Fig. 8 were numerically evaluated, and two typical results are summarized in Fig. 9. The stress intensity factor is shown as a function of the phase angle  $\theta$  (see Fig. 8). The stress intensity factor is shown for the dead and live load stress, as well as the residual stress. The dead and live load  $K$ -value is almost constant along the circumference because of the ratio  $a/c$ . Superimposed is the  $K$ -value resulting from the residual stress field. The stress intensity factors are corrected by the finite width and the free surface correction factor.

The crack front moves into the web and the flange plates as soon as the embedded crack becomes too large to be accommodated in the weld area of the web-flange welded connection. Typical crack stages in the web and flange are shown in Fig. 8 and indicated as E and F. These crack configurations were treated as two independent edge cracks. Both crack fronts (the front in the web and the front in the flange) propagate at the same rate, because the cyclic applied stress is uniform. The total crack opening is almost the same, because the residual stress distribution in the web is almost identical to the stress distribution in the flange. Hence, the crack in the web can be analyzed independent of the crack in the flange.

The analysis of a crack with an irregular crack front and stresses varying over the crack length and plate thickness was made using a numerical procedure. The numerical procedure is based upon the solution of a semiinfinite straight fronted three-dimensional crack. In order to obtain the  $K$ -value for different boundary conditions, the solution has to be normalized by  $1/\pi$  and integrated between  $-\pi/2$  to  $\pi/2$  over the entire crack surface<sup>8</sup>.

$$K = \frac{1}{\pi} \int_0^a \int_{-\pi/2}^{\pi/2} \sigma(a, \theta) d\theta da$$

This equation was evaluated numerically.

The stress intensity factor for the uniformly applied stress ( $\sigma_{LL}$ ,  $\sigma_{DL}$ ) was estimated using the closed form solution. The stress intensity factor due to residual stress was calculated separately. The stress at the box corner was replaced by a splitting force. Numerical results were obtained for the different crack conditions. The total stress intensity factor was obtained by superposition.

#### 4. PREDICTED FATIGUE BEHAVIOR OF THE CRACKS AT THE WELD CORNER

It is of primary importance to know if fatigue crack propagation under the cyclic applied live load will occur for the crack shapes shown in Fig. 8. If fatigue crack growth under the cyclic applied live load stress is likely, then the cracks will increase in size, and brittle fracture could eventually result. If the crack geometry and the applied stress are small enough, no crack growth will occur. Small cracks may be tolerated if the structure's factor of safety is adequate against fracture throughout its service life. In order to establish the reserve against brittle fracture, the dimensions of the largest crack and the fracture toughness of the material has to be known for the lowest anticipated service temperature.

The cracks at the intersection of the web and flange are in a zone of high tensile residual stress. The R-ratio is close to unity which decreases the threshold stress intensity range to a minimum value of  $2.75 \text{ MPa}\sqrt{\text{m}}$ . The usual flaws at the fillet weld root (i.e. pores and slag) have contributed to the formation of transverse cold cracks in the weld. These cracks are irregular in shape, so that locally a higher stress intensity factor may exist. The crack tip is very sharp, because the cracks were caused by cold cracking.

The cyclic applied equivalent Miner stress range was approximated as  $14 \text{ MPa}\sqrt{\text{m}}$  for axial stress and bending. For the crack initiation, the maximum possible stress range under service loads has to be considered. The maximum stress range due to the traffic load was assumed to be  $28 \text{ MPa}$ .

It was found that the stress intensity range is larger than  $\Delta K_{TH}$  for all the crack shapes shown in Fig. 8. Crack shapes B, C and D exceed the crack growth threshold when the stress range is  $14 \text{ MPa}$ . The increase in the total stress intensity factor (due to traffic, dead load and residual stress) is rapid, as the crack approaches the back free surface. Figure 9 shows the stress intensity along the crack front for crack shapes C and D. A material with poor fracture toughness (i.e.  $50$  to  $60 \text{ MPa}\sqrt{\text{m}}$ ) will likely fracture with crack propagation between crack shapes C and D. If the material has better fracture toughness, larger crack sizes can develop before crack instability. Fortunately all cracks were detected and retrofitted before this occurred.

#### 5. RETROFITTING PROCEDURES

The examination of the defects and analysis indicated that it was desirable to grind and inspect with liquid penetrant all manually welded box corners. These locations were suspect, as it was likely that inadequate levels of preheat existed when the manual weld passes were made. Except for the pinned connections, these locations were confined to the bolted splices between the end of a member and the first internal diaphragm.



Fig. 10 Photo Showing Retrofit

All cracks in the longitudinal weldments were removed by either grinding, drilling or coring. Figure 10 shows a retrofitted region after removal of a crack. The ground area was checked by liquid penetrant to ensure that no crack tip remained in the structure.



## 6. CONCLUSIONS

The largest embedded cracks in the web-to-flange connections were found to be susceptible to fatigue crack propagation under the most severe service load conditions. Hence, the cracks in the weldments would enlarge and sharpen with an accumulation of stress cycles if not removed from the structure.

The transverse cracks in the longitudinal web-flange fillet welds were all caused at the time of fabrication. They were all located in manually made sections of the longitudinal weldments. This observation and the fractographic and metallographic examination all suggested these cracks were hydrogen related. All cracks removed from the structure for examination were found to originate at a porosity or entrapped slag and were in a region of high weld shrinkage stress.

The criticality of the transverse cracks were assessed by a fracture mechanics analysis considering the contributions of dead load, live load and welding residual stresses. This permitted the defects to be evaluated and removed in an expeditious manner.

## 7. REFERENCES

- [1] Takahashi, E. and Iwai, K., PREVENTION OF THE TRANSVERSE CRACKS IN HEAVY WELDMENTS OF 2-14/C<sub>r</sub> - 1 M<sub>o</sub> STEEL THROUGH LOW TEMPERATURE POSTWELD HEAT TREATMENT, Transactions of the Japan Welding Society, Vol. 10, No. 1, April 1979.
- [2] Fisher, J. W., et al., FATIGUE AND FRACTURAL RESISTANCE OF LIBERTY BRIDGE MEMBERS, Fritz Engineering Laboratory Report No. 420.2, Lehigh University, Bethlehem, PA, May 1981.
- [3] Fisher, J. W., et al., AN EVALUATION OF THE FRACTURE OF THE I79 BACK CHANNEL GIRDER AND THE ELECTROSLAG WELDS IN THE I79 COMPLEX, Fritz Engineering Laboratory Report No. 425-1(80), Lehigh University, Bethlehem, PA, October 1980.
- [4] Doi, D. A. and Guell, D. L., A DISCRETE METHOD OF THERMAL STRESS ANALYSIS APPLIED TO SIMPLE BEAMS, Appendix IV, Vol. I, NCHRP 12-1 and 12-6, Transportation Research Board, National Research Council, Washington, D.C., October 1974.
- [5] Daniels, J. H. and Batcheler, R. P., FATIGUE OF CURVED STEEL BRIDGE ELEMENTS, EFFECT OF NEXT CURVING ON THE FATIGUE STRENGTH OF PLATE GIRDERS, U. S. Department of Transportation, Federal Highway Administration, DOT-FH-11-8198.5, Washington, D.C., 1972.
- [6] Tall, L., RESIDUAL STRESSES IN WELDED PLATES - A THEORETICAL STUDY, Welding Journal, Vol. 43, American Welding Society, New York City, 1964.
- [7] Tada, H., Paris, P. and Irwin, G. R., THE STRESS ANALYSIS OF CRACKS HANDBOOK, Del Research Corp., Hellertown, PA, 1973.
- [8] Roberts, R., et al., DETERMINATION OF TOLERABLE FLAW SIZE IN FULL SIZE WELDED BRIDGE DETAILS, Report FHWA-RD-77-710, Federal Highway Administration, Office of Research and Development, Washington, D.C., 1977.